2

Comparison of plasma input and reference tissue models for analysing [^{11}C]flumazenil studies

Ursula MH Klumpers, Dick J Veltman, Ronald Boellaard, Emile FI Comans, Cassandra Zuketto, Maqsood Yaqub, Jurgen EM Mourik, Mark Lubberink, Witte JG Hoogendijk, Adriaan A Lammertsma

ABSTRACT

A single tissue compartment model with plasma input is the established method for analysing [^{11}C]flumazenil ([^{11}C]FMZ) studies. However, arterial cannulation and measurement of metabolites are time-consuming. Therefore, a reference tissue approach is appealing, but this approach has not been fully validated for [^{11}C]FMZ.

Methods: Dynamic [^{11}C]FMZ PET scans with arterial blood sampling were performed in nine drug-free depressive patients and eight healthy subjects. Regions of interest were defined on coregistered MRI scans and projected onto dynamic [^{11}C]FMZ images. Using a Hill-type metabolite function, single (1T) and reversible two-tissue (2T) compartmental models were compared. Simplified reference tissue model (SRTM) and full reference tissue model (FRTM) were investigated using both pons and (centrum semiovale) white matter as reference tissue.

Results: The 2T model provided the best fit in 59% of cases. Two-tissue V_T values were on average 1.6% higher than 1T V_T values. Owing to the higher rejection rate of 2T fits (7.3%), the 1T model was selected as plasma input method of choice. SRTM was superior to FRTM, irrespective whether pons or white matter was used as reference tissue. BP_{ND} values obtained with SRTM correlated strongly with 1T V_T (r = 0.998 and r = 0.995 for pons and white matter respectively). Use of white matter as reference tissue resulted in 5.5% rejected fits, primarily in areas with intermediate receptor density. No fits were rejected using pons as reference tissue. Pons produced 23% higher BP_{ND} values than white matter.

Conclusion: For most clinical studies, SRTM with pons as reference tissue can be used for quantifying [^{11}C]FMZ binding.

INTRODUCTION

[^{11}C]Flumazenil (FMZ) is one of the best-characterised positron emission tomography (PET) ligands. It is a selective, reversibly bound, high-affinity neutral antagonist of the benzodiazepine site of the ɣ-aminobutyric acid ($GABA_A$)- receptor, showing rapid uptake and a high specific to nonspecific binding ratio in human brain (1). Neither of its two labelled hydrophilic metabolites in human plasma, [^{11}C]Ro 15-3890 and [^{11}C]Ro 15-7965, cross the blood-brain barrier and therefore the PET signal is solely due to [^{11}C]FMZ (2).

Previous studies (3-5) have shown that kinetics of [^{11}C]FMZ binding can best be quantified using the total volume of distribution V_T, obtained using a single-tissue compartment model with plasma input. Although V_T contains a nonspecific component, it has been estimated that this is of the order of 10% (5,6), at least within the normal brain.

In evaluating [^{11}C]FMZ binding, the majority of clinical brain studies (7-11) have used parametric approaches, mainly spectral analysis (12) or pixel-by-pixel weighted integration (13), depicting cerebral ligand transport and receptor binding.

Clearly, when evaluating the effects of therapy, [^{11}C]FMZ studies should be analysed using the most accurate tracer kinetic model. Although both aforementioned methods simplify the computations, they do not obviate the need for arterial cannulation, nor exclude the workload associated with measuring plasma metabolites.

As a result, in practice, studies using a reference tissue approach have been reported (14-17). Both pons and white matter have been proposed as reference tissues (14,18), but both can be criticised. The pons is a small structure, which might have partial volume effects. In addition, it has been stated that the pons is not totally devoid of receptors (5,6,19,20) On the other hand, centrum semiovale white matter could have spill-over from cortical grey matter radioactivity. It can be questioned whether the level of nonspecific binding is the same in grey and white matter, a requirement for the use of reference tissue models (21). Therefore, the main purpose of the present study was to assess whether use of a reference tissue model would be an option for analysing clinical [^{11}C]FMZ studies. This assessment requires a comparison with the optimal plasma input model.

MATERIALS AND METHODS

Subjects

Nine drug-free patients (4 men; mean age ± SD 39 ± 11, range 23 to 54 years) with a major depressive episode according to DSM-IV (22) were recruited from an outpatient psychiatric clinic. Patients were age-matched with eight healthy control subjects without present or past history of psychiatric illness (5 men, mean age 32 ± 8, range 22 to 42 years).

Informed consent was obtained from all participants. The study protocol was approved by the medical ethics committee of the VU University Medical Center. Subjects were excluded if they suffered from somatic disorders or used drugs that are known to interfere with the GABAergic system, including benzodiazepines, psychoactive drugs and alcohol abuse. Patients had to be free of antidepressants and benzodiazepines for at least 3 months and 2 weeks, respectively, at the time of PET scanning. Six patients were drug naive and had their first major depression. All patients and controls had standard physical and laboratory examinations.

Scan protocol

Prior to scanning, an arterial line was inserted into a radial artery under local anesthesia (xylocaine 1%, 1 mL). Subjects were then transferred to the scanner room and studied at rest, in supine position, with ears unplugged using an ECAT EXACT HR+ scanner (Siemens/CTI, Knoxville, TN, USA). First, a 10 min two-dimensional (2D) transmission scan was acquired using rotating ^{68}Ge/^{68}Ga sources. This scan was used to correct the subsequent emission scan for tissue attenuation. Next, a dynamic three-dimensional (3D) scan (16 frames with progressively increasing frame length) with a total duration of 60 min was acquired, after bolus injection of 370 ± 45 MBq [^{11}C]FMZ with a specific activity of 62 ± 20 GBq/µmol.

During the scan, arterial whole blood was monitored continuously using an on-line detection system (23). In addition, discrete samples were taken at 2.5, 5, 10, 20, 30, 40 and 60 min. These were used for calibrating the (on-line) blood sampler, for measuring plasma/whole-blood ratios, and for determining metabolite fractions, enabling the generation of a metabolite-corrected plasma input curve. Fractional concentrations of hydrophilic metabolites and unchanged (lipophilic) [^{11}C]FMZ were determined by solid phase extraction of plasma followed by high-performance liquid chromatography (HPLC) (24). All subjects underwent a T1-weighted structural MRI scan, using a 1.5T Sonata MR system (Siemens, Erlangen, Germany).

Image processing

Images were reconstructed using FORE+ 2D filtered back projection (FBP), applying a Hanning filter with a cut-off at 0.5 of the Nyquist frequency. Images consisted of 63 planes of 256 x 256 voxels of 1.2 x 1.2 x 2.4 mm^3 with a reconstructed image resolution of approximately 7 mm. Image analysis was performed with CAPP software provided by the manufacturer (Siemens/CTI, Knoxville, TN, USA) on SUN workstations (Sun Microsystems, Mountain View, CA, USA). First, magnetic resonance imaging (MRI) scans were coregistered with summed [^{11}C]FMZ images (10-60 min p.i.) (25,26). Next, regions of interest (ROIs) were manually defined on these coregistered MRI scans on consecutive planes, in cranial-caudal order, starting with the plane in which the diameter of the cerebrum no longer increased in width and ending in the plane where either the cerebellum or the temporal poles were no longer visible, using the anatomical atlas of Duvernoy et al. (27). The following structures were included: anterior, ventrolateral, dorsolateral and orbitomedial prefrontal cortex, anterior and posterior cingulate, medial and lateral temporal lobe and insular area, parietal and occipital area, cerebellum, hippocampus, putamen, thalamus. Pons and centrum semiovale white matter were selected as reference tissue ROIs (Figure 1). In the remainder of this article, centrum semiovale white matter will be denoted as white matter.

Finally, ROIs were projected onto the dynamic [^{11}C]FMZ images, generating time activity curves for each region.

Figure 1

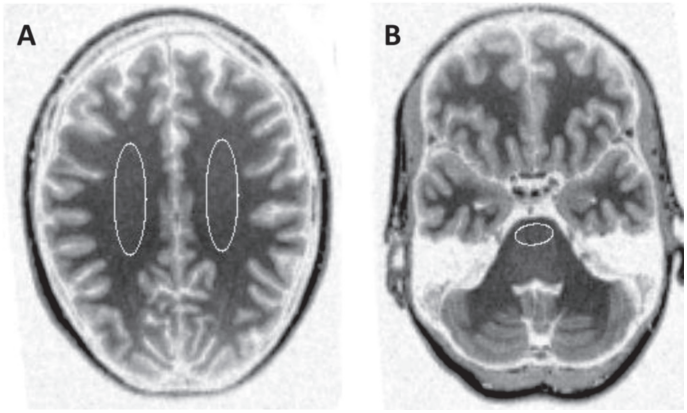

Examples of reference tissue ROIs for (A) centrum semiovale white matter and (B) pons. For centrum semiovale white matter elliptical ROIs were drawn bilaterally on two consecutive planes, for pons elliptical ROIs were drawn on three consecutive planes.

Fitting procedure

Nonlinear least-squares fits were performed using the f_{mins} function as included in the Matlab 5.3 optimization toolbox (The Mathworks, Natick, MA, USA), applying the Nelder-Mead simplex method, with a maximum number of function evaluations of 400 times the number of parameters and a termination tolerance of 10^{-4}.

Data analysis

Plasma input models

To derive a metabolite-corrected input function from the measured whole-blood curve, the metabolite data obtained from the discrete samples need to be interpolated by fitting an appropriate function to these data. In most studies, a multi-exponential function has been used. The main problem associated with a multi-exponential function is the rather poor description of early time points, where the multi-exponential is 'steeper' than the actual ingrowth of labelled metabolites (28). A more physiologic description of the early time course of these metabolites is given by a Hill function, as first demonstrated by Gunn et al. (29) for [carbonyl-^{11}C]WAY-100635. The Hill function describes the metabolite fraction data *m(t)* by:

$$m(t) = \frac{\alpha t^{\beta}}{t^{\beta} + \gamma}$$

where α, β and γ are fit parameters, and *t* is the time after injection. Recently, simulations indicated improved accuracy and precision for V_T of [^{11}C]FMZ when using a Hill function rather than a multi-exponential (30).

A change in metabolite correction will affect the final-derived metabolite-corrected plasma input function and, consequently, also both single- (1T) and two-tissue (2T) fits, potentially affecting the relative preference of both models. Therefore, in this study, a formal comparison between 1T (two rate constants) and 2T (four rate constants) models (both with an additional parameter for blood volume) was repeated. Because of the large variability in binding potential (BP_{ND}), together with the presence of many nonphysiologic values, V_T was also chosen as parameter of outcome for the 2T model.

For the comparison of 1T and 2T model fits, only data that fulfilled strict quality control criteria were used. V_T results for either model were not used when the (fitted) standard

error of V_T was larger than 25% or when the fit did not converge. The cut-off value of 25% was chosen arbitrarily. The number of rejected fits was, however, insensitive to the actual cut-off value used. Changing this value from 25 to 50% had no effect on the 1T model and decreased the number of rejected fits for the 2T model by only 0.7%. If V_T values were available for both 1T and 2T models, they were compared using Akaike (31) and Schwarz (32) criteria. Final assessment was based on both acceptance rate and Akaike/Schwarz criteria.

Reference tissue models

Both full reference tissue model (FRTM, four parameters (33,34)) and simplified reference tissue model (SRTM, three parameters (21)) were investigated using both pons and (centrum semiovale) white matter as reference tissues.

The comparison between FRTM and SRTM was performed in an identical manner as for the 1T and 2T models, except that for the reference tissue models BP_{ND} (rather than V_T) was used as the parameter of interest.

Finally, 1T and 2T models were compared with SRTM and FRTM using correlation analysis.

RESULTS

Plasma input models

Figure 2 shows a typical example of plasma metabolite fits using multi-exponential (Figure 2A) and Hill (Figure 2B) functions. It is clear that the Hill function provides a significantly better fit through the metabolite data, especially at early time points. According to the Akaike criterion, the Hill function yielded significantly better metabolite fits than the multi-exponential function for all subjects (mean Akaike number -50 versus -28, respectively; p <0.0001). Therefore, in the remainder of this study only the Hill function was used to fit the metabolite data.

According to Akaike and Schwarz criteria alone, the 1T model was preferred in 38% of the fits across all structures (and subjects) investigated (Table 1). For structures with minor (white matter, pons) or intermediate (thalamus, putamen) levels of receptors, there was a stronger preference for the 1T model.

Figure 2

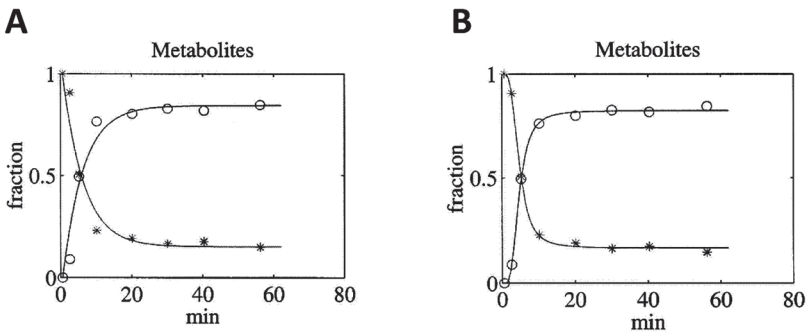

Typical [^{11}C]FMZ metabolite fits using (A) multi-exponential and (B) Hill function fits. Measured [^{11}C]FMZ parent (= *) and metabolite (= o) fractions are plotted as function of time post injection, with lines representing best fits.

All 1T fits were of satisfactory quality and none had to be rejected. In contrast, 21 of the 272 2T fits (i.e. 7.3%; Table 1) fulfilled the rejection criteria, with a slightly higher number of rejections in the patient group (15) than in the normal controls (6). When left and right hemisphere data were analysed independently, similar rejection rates were observed (data not shown). When Akaike and Schwarz results were corrected for rejected fits, the 1T model was preferred in 41% of the fits (across structures and subjects) and the 2T model in 59%.

Average (± SD) V_T values for the various structures, obtained with both 1T and 2T model fits, are shown in Table 2. To compare methods, only those V_T values were used where both 1T and 2T models provided reliable fits (ratio 2T/1T). V_T values obtained with the 2T model were on average 1.6% higher than those obtained with the 1T model (Table 2) with a strong linear correlation between the two (Figure 3). Data from depressive subjects and healthy controls were pooled, as for none of the ROIs significant differences in V_T and BP_{ND} between major depression and healthy controls were encountered.

Reference tissue models

According to Akaike and Schwarz criteria alone, SRTM was preferred over FRTM in 89 and 79% of the fits across all structures, when using pons and white matter as reference tissue, respectively (Tables 3A and 3B).

Table 1: Comparison of 1T and 2T models

	Preference according to Akaike / Schwarz criteria				Cumulative rejections				Best fit			
Structure	**1T n**	**1T %**	**2T n**	**2T %**	**1T total**	**2T co**	**2T pat**	**2T total**	**1T n**	**1T %**	**2T n**	**2T %**
Lat Temporal	4	24	13	76	0	0	1	1	4	24	13	76
Med Temporal	5	29	12	71	0	0	1	1	5	29	12	71
Insula	7	41	10	59	0	0	2	2	7	41	10	59
Ant Prefrontal	6	35	11	65	0	1	2	3	8	47	9	53
VL Prefrontal	6	35	11	65	0	0	1	1	6	35	11	65
DL Prefrontal	8	47	9	53	0	0	0	0	8	47	9	53
OM Prefrontal	3	18	14	82	0	1	1	2	5	29	12	71
Ant Cingulate	6	35	11	65	0	1	1	2	7	41	10	59
Post Cingulate	5	29	12	71	0	1	2	3	8	47	9	53
Parietal	4	24	13	76	0	0	1	1	5	29	12	71
Occipital	5	29	12	71	0	0	0	0	5	29	12	71
Cerebellum	3	18	14	82	0	0	0	0	3	18	14	82
Hippocampus	2	12	15	88	0	0	1	1	2	12	15	88
Thalamus	11	65	6	35	0	1	0	1	11	65	6	35
Putamen	12	71	5	29	0	1	2	3	13	76	4	24
Pons	12	71	5	29	0	0	0	0	12	71	5	29
White Matter	10	59	7	41	0	0	0	0	10	59	7	41
Total (n)	109		180		0	6	15	21	119		170	
Average (%)		38		62				7.3		41		59

Ant, anterior; co, controls; DL, dorsolateral; Lat, lateral; Med, medial; OM, orbitomedial; pat, patients with major depressive disorder; Post, posterior; VL, ventrolateral.

SRTM with pons as reference tissue resulted in no unreliable BP_{ND} values. In contrast, for FRTM with pons as reference tissue, the percentage of unreliable BP_{ND} values was 51.7% ($n = 52$ in patients, $n = 80$ in controls), spread over all structures (data not shown). Almost similar results were obtained when white matter was used as reference tissue, except that here also 5.5% of fits were rejected for SRTM. These rejected fits were related to deep grey matter structures, that is thalamus (10) and putamen (4) in both subject groups. In this case the rejection rate for FRTM was 42.7%, virtually equally spread over patients and controls, and affecting all structures (data not shown).

Table 2: Average V_T ± SD values for 1T and 2T plasma input models

Structure	1T	2T	Ratio 2T/1T[a]
Lat Temporal	5.31 ± 0.48	5.41 ± 0.42	1.02
Med Temporal	4.69 ± 0.49	4.83 ± 0.46	1.02
Insula	5.80 ± 0.63	5.93 ± 0.53	1.02
Ant Prefrontal	4.36 ± 0.47	4.44 ± 0.43	1.00
VL Prefrontal	5.18 ± 0.45	5.26 ± 0.42	1.02
DL Prefrontal	5.19 ± 0.56	5.24 ± 0.52	1.01
OM Prefrontal	5.46 ± 0.48	5.60 ± 0.49	1.02
Ant Cingulate	5.29 ± 0.63	5.42 ± 0.62	1.01
Post Cingulate	4.87 ± 0.64	5.03 ± 0.62	1.01
Parietal	5.05 ± 0.64	5.09 ± 0.57	1.02
Occipital	5.63 ± 0.68	5.63 ± 0.59	1.01
Cerebellum	4.21 ± 0.37	4.26 ± 0.31	1.01
Hippocampus	3.10 ± 0.49	3.26 ± 0.52	1.04
Thalamus	2.71 ± 0.38	2.64 ± 0.33	1.00
Putamen	2.95 ± 0.34	3.00 ± 0.33	0.99
Pons	0.84 ± 0.13	0.86 ± 0.14	1.03
White Matter	0.97 ± 0.14	1.00 ± 0.13	1.04
average			1.02

Ant, anterior; DL, dorsolateral; Lat, lateral; Med, medial; OM, orbitomedial; pat, patients with major depressive disorder; Post, posterior; SD, standard deviation; VL, ventrolateral. [a]Ratio 2T/1T if corrected for inferior fits.

Figure 3

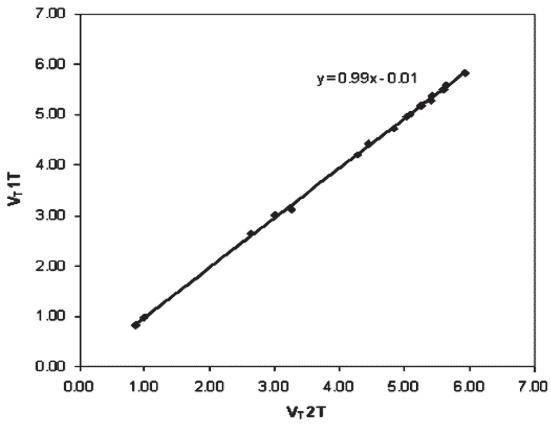

Comparison of V_T values for each of the bilateral ROIs, averaged across all 17 subjects, obtained using 1T and 2T plasma input models. The line represents the linear regression between the two data sets (r = 0.999; p = 0.01).

When data from Akaike and Schwarz criteria were corrected for rejected fits, SRTM was preferred over FRTM in 96% of fits, when pons was used as reference tissue. For white matter as reference tissue, SRTM was preferred over FRTM in 76% of cases. In 5.5%, however, neither SRTM nor FRTM provided an adequate fit.

BP_{ND} results with both pons and white matter as reference tissue are listed in Tables 3A and 3B. On average, pons produced 23% higher BP_{ND} values than white matter (Figure 4).

Figure 4

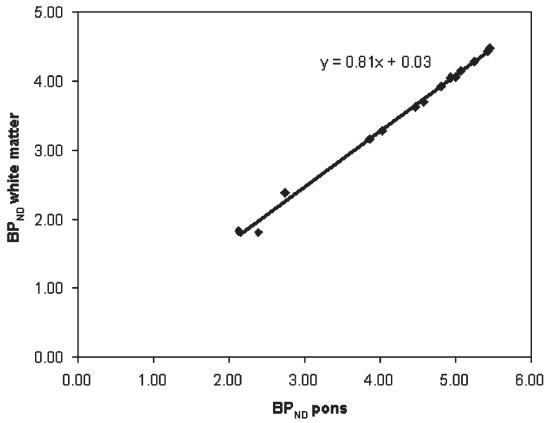

Comparison of BP_{ND} values for each of the bilateral ROIs, averaged across all 17 subjects, obtained with SRTM using both pons and centrum semiovale white matter as reference tissue. The line represents the linear regression between the two data sets (r = 0.997; p = 0.01). BP_{ND} using pons as reference tissue was on average 23% higher than BP_{ND} using white matter as reference tissue.

Reference tissue versus plasma input models

Based on the findings of the previous sections, BP_{ND} values obtained with SRTM were compared with V_T values obtained with the 1T plasma input model. Figure 5 shows the results of this comparison, where both pons and white matter were used as reference tissue for SRTM. The figure illustrates the higher BP_{ND} values obtained with pons as reference tissue. The correlation between BP_{ND} and V_T, however, was similar when data were corrected for rejected fits (higher number in case of white matter as reference tissue).

In this study, Pearson correlations between BP_{ND} from SRTM and V_T from the 1T model were highly significant, being 0.998 using pons, and 0.995 for white matter as reference tissue, respectively. For the 2T model these were identical. The slightly higher rejection rate for the latter should, however, be kept in mind.

Table 3A: Selection criteria evaluating SRTM (versus FRTM), using pons as reference tissue

	Preference according to Akaike / Schwarz criteria		Rejections	Best fit		BP_{ND} ± SD
Structure	**n**	**%**	**n**	**n**	**%**	
Lat Temporal	16	94	0	17	100	5.08 ± 1.16
Med Temporal	14	82	0	16	94	4.48 ± 1.02
Insula	14	82	0	14	82	5.46 ± 1.19
Ant Prefrontal	14	82	0	17	100	4.03 ± 0.91
VL Prefrontal	16	94	0	17	100	4.93 ± 1.05
DL Prefrontal	14	82	0	16	94	4.94 ± 1.08
OM Prefrontal	16	94	0	17	100	5.25 ± 1.12
Ant Cingulate	16	94	0	16	94	5.00 ± 1.21
Post Cingulate	17	100	0	17	100	4.58 ± 1.29
Parietal	14	82	0	17	100	4.81 ± 1.14
Occipital	15	88	0	17	100	5.43 ± 1.30
Cerebellum	17	100	0	17	100	3.87 ± 0.94
Hippocampus	13	76	0	13	76	2.75 ± 0.76
Thalamus	14	82	0	16	94	2.14 ± 0.52
Putamen	17	100	0	17	100	2.39 ± 0.64
%		89	0		96	

Ant, anterior; BP_{ND}, binding potential; DL, dorsolateral; FRTM, full reference tissue model; OM, orbitomedial; Post, posterior; SRTM, simplified reference tissue model; SD, standard deviation; VL, ventrolateral.

Table 3B: Selection criteria evaluating SRTM (versus FRTM), using centrum semiovale white matter as reference tissue

	Preference according to Akaike / Schwarz criteria		Rejections	Best fit		BP_{ND} ± SD
Structure	**n**	**%**	**n**	**n**	**%**	
Lat Temporal	16	94	0	16	94	4.15 ± 0.71
Med Temporal	15	88	0	15	88	3.63 ± 0.67
Insula	12	71	0	12	71	4.48 ± 0.87
Ant Prefrontal	13	76	0	13	76	3.28 ± 0.77
VL Prefrontal	14	82	0	14	82	4.04 ± 0.79
DL Prefrontal	14	82	0	14	82	4.06 ± 0.80
OM Prefrontal	14	82	0	14	82	4.28 ± 0.74
Ant Cingulate	14	82	0	14	82	4.06 ± 0.65
Post Cingulate	14	82	0	14	82	3.70 ± 0.76
Parietal	15	88	0	15	88	3.92 ± 0.75
Occipital	13	76	0	14	82	4.43 ± 0.77
Cerebellum	13	76	0	13	76	3.16 ± 0.59
Hippocampus	8	47	0	9	53	2.38 ± 0.76
Thalamus	15	88	10	7	41	1.83 ± 0.50
Putamen	12	71	4	10	59	1.81 ± 0.40
%		79	5.5		76	

Ant, anterior; BP_{ND}, binding potential; DL, dorsolateral; FRTM, full reference tissue model; OM, orbitomedial; Post, posterior; SRTM, simplified reference tissue model; SD, standard deviation; VL, ventrolateral.

Figure 5

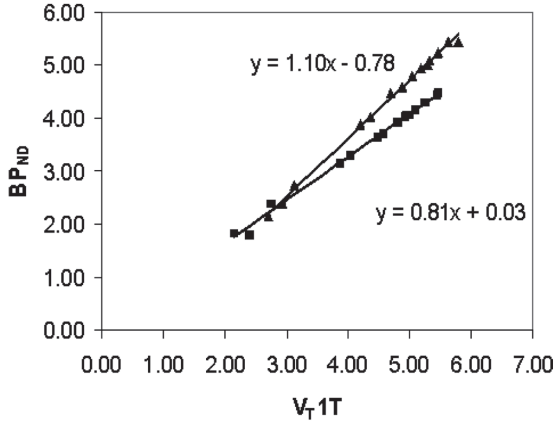

Relationship between V_T 1T and BP_{ND} SRTM for pons and centrum semiovale white matter. Individual values represent bilateral ROIs, averaged across all 17 subjects. The upper line represents the linear regression for pons (r = 0.998; p = 0.01), the lower line for white matter (r = 0.995; p = 0.01). No fits were rejected in using pons as reference tissue. Use of white matter as reference tissue resulted in 5.5% rejected fits.

DISCUSSION

[^{11}C]Flumazenil kinetics have been described extensively in the original report by Pappata et al. (35) and in a number of subsequent studies (3-6,20,36).

The main purpose of this study was not to readdress [^{11}C]FMZ kinetics, but to assess whether reference tissue methods could be used for analysing [^{11}C]FMZ studies. This assessment requires a comparison with the optimal plasma input model. Previously, it has been shown that [^{11}C]FMZ kinetics are best described by a 1T compartment model (4,5). Recently, however, it was shown that the ingrowth of labelled metabolites into plasma is best described by a Hill function (30). This was further confirmed in the present study, where metabolites were better fitted using a Hill function than using a multi-exponential (Figure 2). As previously simple interpolation and multi-exponential fits were used, these methods could have affected the quality of both 1T and 2T model fits and thereby also the relative preference between the two models. Therefore, the comparison of 1T and 2T models was repeated in the present study.

Both cortical and subcortical areas were investigated. To increase statistical power, data from depressive subjects and controls were pooled. This is justified, as no significant differences between depressive patients and healthy controls were observed for any of the ROIs investigated, in line with findings reported by Kugaya et al. (37). In addition, within the group of depressed patients, no relationship between severity of depression and either V_T or BP_{ND} was found (data not shown).

In apparent contrast to previous studies (4,5), after correcting for inferior fits, the 1T model was preferred in 41% of the fits and the 2T model in 59%, slightly favouring the 2T model. Owing to a sharp increase in coefficients of variation of fit parameters with increasing model complexity (20 to 50% for a three-parameter model and 50 to 100% for a four-parameter model), coupled with a nonsignificant improvement in goodness of fit, Koeppe et al. (4) preferred the 1T model. Only for regions with low receptor density, where free and nonspecific binding constitute a greater fraction of V_T, the 2T model was implied to be superior. This latter finding could not be substantiated in the present study, as the 1T model was actually preferred for deep grey matter structures with intermediate levels of receptors density.

Despite a slight preference for the 2T method in case of successful fits, its 7.3% failure rate, together with the very small difference between 1T and 2T V_T values (1.6%), implies that the 1T model seems to be the method of choice for routine clinical studies, in line with previous studies.

It should be noted that a systematic difference between 1T and 2T models was observed, albeit small. This might have implications for techniques that automatically select the number of compartments in voxel-by-voxel analyses, such as spectral analysis (12). The 2T model was selected most often for regions with high, and less for regions with low receptor densities (Table 1). This could mean that, within-group comparisons or when monitoring response to therapy, a reduction in receptor density will be overestimated (for higher densities the higher 2T V_T would be favoured and for lower densities the lower 1T V_T). Although effects would be small for [^{11}C]FMZ, they should be taken into account for tracers where the differences in V_T are larger.

With respect to reference tissue models it is clear that SRTM was superior to FRTM, irrespective whether pons or (centrum semiovale) white matter was used as reference

tissue. The high failure rate of FRTM is not surprising as it is based on the existence of two distinct tissue compartments. The plasma input models already indicated that this distinction is small, if not absent, given the good performance of the 1T model.

Pons and white matter have previously been considered as reference regions with very low or negligible benzodiazepine receptor densities, respectively (12,14,18,36,38,39). *In vitro* studies on rat brain slices have indicated that the brain stem is not entirely free of receptors (40), which was confirmed in *in vivo* studies (5,6,41). Although the spherical properties of the pons limit partial volume effect due to contamination with cortical grey matter, it is also a small structure, potentially underestimating radioactivity concentration because of limited spatial resolution of PET. Moreover, pons comprises pontine grey matter nuclei. The ventral side of the pons, however, includes the ventral tegmentum, consisting of (white) axonal fibers. By defining the pons ROI on the ventral side of the pons, an attempt was made to minimise the effects of grey matter 'contamination'. It should be noted that, due to its small size, measured radioactivity concentrations especially in pons might be sensitive to even small patient movements, consequently affecting quantification. Therefore, care should be taken in minimising patient movement and, if required, appropriate movement corrections should be implemented.

To exclude potential effects of patient movement on the present results, all scans were checked for subject movement retrospectively. The majority of studies did not show observable displacement. Only for one patient, significant movement, that is a 12-mm translation in the cranial-caudal direction was observed. To assess the impact on quantification, this study was corrected for movement using a frame-by-frame realignment procedure. After movement correction, regional V_T and BP_{ND} values changed with, on average, 1 and 9%, respectively. Pearson correlation remained unaltered, being $r = 0.998$ for 1T V_T and SRTM BP_{ND}. As even for this most extreme case, the impact of patient movement on regional V_T and BP_{ND} values was still small, it may be assumed that overall effects of patient movement on V_T and BP_{ND} results in the present study are minimal.

This conclusion may be extended to partial volume effects, given the excellent correlation between BP_{ND} obtained with pons as reference tissue input and V_T obtained with plasma input (i.e. without using the pons).

Finally, a potential limitation of the use of white matter as reference tissue is the inherent assumption that the levels of nonspecific binding are identical in grey and white matter. The results of the present study are in favour of using pons rather than white matter as reference tissue. Firstly, pons resulted in no unsatisfactory fits. In contrast, white matter resulted in a small fraction (5.5%) of unsatisfactory fits, primarily for some deep grey matter structures. Secondly, pons used as reference tissue yielded BP_{ND} values that were on average 23% higher than those obtained with white matter. This suggests a higher level of specific or (more likely) nonspecific binding in white matter, which corresponds to the higher V_T value for white matter than for pons (Table 2; 1T plasma input model).

The results presented here are in line with those of Abadie et al. (14) who compared pons, hemispheric white matter and corpus callosum as reference tissue structures. Abadie et al. (14), however, employed a pseudo-equilibrium paradigm with B_{max} and K_d as measures of central benzodiazepine receptor density and affinity, whereas here a dynamic approach with V_T as parameter of interest was used. Nevertheless, it is reassuring that both methods favour the pons as reference structure.

Clearly, the most important question is whether a reference tissue rather than a plasma input model could be used. Based on excellent correlation (r = 0.998) between SRTM and the 1T plasma input model (Figure 5), this is certainly the case for the present study population, a mixture of normal controls and patients with depression. Correlations within any single subject may even have been higher (4), due to variability in free and nonspecific distribution volumes across subjects.

It should be noted that, despite the good correlation between SRTM and 1T plasma input models, both have their limitations. Firstly, accuracy of SRTM results may be compromised by above-mentioned partial volume effects, and by the low level of central benzodiazepine receptors observed in the pons (5). Although, in theory, it should be possible to take into account this specific binding in pons using an extended reference tissue model (42), for FMZ this is not possible in practice yet, as it would require an independent assessment of the level of specific binding in the pons. Secondly, V_T results obtained using the 1T model include nonspecific binding. This will result in an increasing bias for decreasing levels of central benzodiazepine receptors. From Figure 5 it can be deduced that, in the present study, the level of nonspecific binding is around 12%, which is virtually similar to earlier reports (5,20,36).

In conclusion, for clinical studies, a simplified reference tissue model with pons as reference tissue can be used for quantification of [^{11}C]FMZ binding. This obviates the need for arterial cannulation and significantly simplifies the scanning protocol.

ACKNOWLEDGMENTS

The authors thank the PET radiochemistry and technologists staff of the Division of Nuclear Medicine & PET Research for production of isotopes and acquisition of PET and metabolites data.

REFERENCES

1. Samson Y, Hantraye P, Baron JC, Soussaline F, Comar D, Maziere M (1985): Kinetics and displacement of [^{11}C]RO 15-1788, a benzodiazepine antagonist, studied in human brain in vivo by positron tomography. *Eur J Pharmacol* 110:247-51.
2. Debruyne D, Abadie P, Barre L, Albessard F, Moulin M, Zarifian E, et al. (1991): Plasma pharmacokinetics and metabolism of the benzodiazepine antagonist [^{11}C] Ro 15-1788 (flumazenil) in baboon and human during positron emission tomography studies. *Eur J Drug Metab Pharmacokinet* 16:141-52.
3. Holthoff VA, Koeppe RA, Frey KA, Paradise AH, Kuhl DE (1991): Differentiation of radioligand delivery and binding in the brain: validation of a two-compartment model for [^{11}C]flumazenil. *J Cereb Blood Flow Metab* 11:745-52.
4. Koeppe RA, Holthoff VA, Frey KA, Kilbourn MR, Kuhl DE (1991): Compartmental analysis of [^{11}C]flumazenil kinetics for the estimation of ligand transport rate and receptor distribution using positron emission tomography. *J Cereb Blood Flow Metab* 11:735-44.
5. Lassen NA, Bartenstein PA, Lammertsma AA, Prevett MC, Turton DR, Luthra SK, et al. (1995): Benzodiazepine receptor quantification in vivo in humans using [^{11}C]flumazenil and PET: application of the steady-state principle. *J Cereb Blood Flow Metab* 15:152-65.
6. Delforge J, Pappata S, Millet P, Samson Y, Bendriem B, Jobert A, et al. (1995): Quantification of benzodiazepine receptors in human brain using PET, [^{11}C]flumazenil, and a single-experiment protocol. *J Cereb Blood Flow Metab* 15:284-300.
7. Hammers A, Koepp MJ, Hurlemann R, Thom M, Richardson MP, Brooks DJ, et al. (2002): Abnormalities of grey and white matter [^{11}C]flumazenil binding in temporal lobe epilepsy with normal MRI. *Brain* 125:2257-71.
8. Koepp MJ, Hammers A, Labbe C, Woermann FG, Brooks DJ, Duncan JS (2000): [^{11}C]Flumazenil PET in patients with refractory temporal lobe epilepsy and normal MRI. *Neurology* 54:332-9.
9. Lloyd CM, Richardson MP, Brooks DJ, Al-Chalabi A, Leigh PN (2000): Extramotor involvement in ALS: PET studies with the $GABA_A$ ligand [^{11}C]flumazenil. *Brain* 123:2289-96.
10. Malizia AL, Cunningham VJ, Bell CJ, Liddle PF, Jones T, Nutt DJ (1998): Decreased brain $GABA_A$-benzodiazepine receptor binding in panic disorder: preliminary results from a quantitative PET study. *Arch Gen Psychiatry* 55:715-20.
11. Richardson MP, Friston KJ, Sisodiya SM, Koepp MJ, Ashburner J, Free SL, et al. (1997): Cortical grey matter and benzodiazepine receptors in malformations of cortical development. A voxel-based comparison of structural and functional imaging data. *Brain* 120:1961-73.
12. Cunningham VJ, Jones T (1993): Spectral analysis of dynamic PET studies. *J Cereb Blood Flow Metab* 13:15-23.
13. Frey KA, Holthoff VA, Koeppe RA, Jewett DM, Kilbourn MR, Kuhl DE (1991): Parametric in vivo imaging of benzodiazepine receptor distribution in human brain. *Ann Neurol* 30:663-72.

14. Abadie P, Baron JC, Bisserbe JC, Boulenger JP, Rioux P, Travere JM, et al. (1992): Central benzodiazepine receptors in human brain: estimation of regional Bmax and KD values with positron emission tomography. *Eur J Pharmacol* 213:107-15.

15. Abadie P, Boulenger JP, Benali K, Barre L, Zarifian E, Baron JC (1999): Relationships between trait and state anxiety and the central benzodiazepine receptor: a PET study. *Eur J Neurosci* 11:1470-8.

16. Bouvard S, Costes N, Bonnefoi F, Lavenne F, Mauguiere F, Delforge J, et al. (2005): Seizure-related short-term plasticity of benzodiazepine receptors in partial epilepsy: a [^{11}C]flumazenil-PET study. *Brain* 128:1330-43.

17. Lucignani G, Panzacchi A, Bosio L, Moresco RM, Ravasi L, Coppa I, et al. (2004): $GABA_A$ receptor abnormalities in Prader-Willi syndrome assessed with positron emission tomography and [^{11}C]flumazenil. *NeuroImage* 22:22-8.

18. Persson A, Pauli S, Halldin C, Stone-Elander S, Farde L, Sjögren I, et al. (1989): Saturation analysis of specific [^{11}C]Ro 15-1788 binding to the human neocortex using positron emission tomography. *Human Psychopharmacology* 4:21-31.

19. Lammertsma AA, Lassen NA, Prevett MC, Bartenstein PA, Turton DR, Luthra SK, et al. Quantification of benzodiazepine receptors in vivo using [^{11}C]flumazenil: application of the steady state principle. In: Uemara K, Lassen NA, Jones T, Kanno I, editors. Quantification of brain function: Tracer Kinetics and Image Analysis in Brain PET.Amsterdam: Excerpta Medica; 1993. p. 303-11.

20. Millet P, Graf C, Buck A, Walder B, Ibanez V (2002): Evaluation of the reference tissue models for PET and SPECT benzodiazepine binding parameters. *NeuroImage* 17:928-42.

21. Lammertsma AA, Hume SP (1996): Simplified reference tissue model for PET receptor studies. *NeuroImage* 4:153-8.

22. Diagnostic Statistic Manual of mental disorders. IV ed. Washington DC: American Psychiatric Association; 1994.

23. Boellaard R, Van Lingen A, Van Balen SC, Hoving BG, Lammertsma AA (2001): Characteristics of a new fully programmable blood sampling device for monitoring blood radioactivity during PET. *Eur J Nucl Med* 28:81-9.

24. Luthra SK, Osman S, Turton DR, Vaja V, Dowsett K (1993): An automated system based on solid phase extraction and HPLC for the routine determination in plasma of unchanged [^{11}C]deprenyl, [^{11}C]deprenorphine, [^{11}C]flumazenil, [^{11}C]raclopride and [^{11}C]Schering 23390. *J Labelled Comp Radiopharm* 32:518-20.

25. Maes F, Collignon A, Vandermeulen D, Marchal G, Suetens P (1997): Multimodality image registration by maximization of mutual information. *IEEE Trans Med Imaging* 16:187-98.

26. West J, Fitzpatrick JM, Wang MY, Dawant BM, Maurer CR, Jr., Kessler RM, et al. (1997): Comparison and evaluation of retrospective intermodality brain image registration techniques. *J Comput Assist Tomogr* 21:554-66.

27. Duvernoy HM, Bourgouin P, Cabanis EA, Cattin F, Guyot J, Iba-Zizen MT, et al. The Human Brain: surface, three-dimensional sectional anatomy with MRI and blood supply. 2nd ed. New York: Springer-Verlag-Wien; 1999.

28. Lammertsma AA, Hume SP, Bench CJ, Luthra SK, Osman S, Jones T. Measurement of monoamine oxidase B activity using L-[^{11}C]deprenyl: Inclusion of compartmental analysis of plasma metabolites and an new model not requiring measurement of plasma metabolites. In: Uemara K, Lassen NA, Jones T, Kanno I, editors. Quantification of brain function: Tracer Kinetics and Image Analysis in Brain PET.Amsterdam: Excerpta Medica; 1993. p. 313-8.

29. Gunn RN, Sargent PA, Bench CJ, Rabiner EA, Osman S, Pike VW, et al. (1998): Tracer kinetic modeling of the 5-HT$_{1A}$ receptor ligand [carbonyl-^{11}C]WAY-100635 for PET. *NeuroImage* 8:426-40.

30. Lubberink M, Greuter HNJM, Boellaard R, Luurtsema G, Lammertsma AA. Effect of plasma metabolite correction accuracy on kinetic analysis in positron emission tomography (2004): *NeuroImage* 22:T119.

31. Akaike H (1974): A new look at the statistical model identification. *IEEE Trans Automat Contr* 19:716-23.

32. Schwarz G (1978): Estimating the dimension of a model. *Ann Statist* 6:461-4.

33. Hume SP, Myers R, Bloomfield PM, Opacka-Juffry J, Cremer JE, Ahier RG, et al. (1992): Quantification of [^{11}C]labeled raclopride in rat striatum using positron emission tomography. *Synapse* 12:47-54.

34. Lammertsma AA, Bench CJ, Hume SP, Osman S, Gunn K, Brooks DJ, et al. (1996): Comparison of methods for analysis of clinical [^{11}C]raclopride studies. *J Cereb Blood Flow Metab* 16:42-52.

35. Pappata S, Samson Y, Chavoix C, Prenant C, Maziere M, Baron JC (1988): Regional specific binding of [^{11}C]RO 15-1788 to central type benzodiazepine receptors in human brain: quantitative evaluation by PET. *J Cereb Blood Flow Metab* 8:304-13.

36. Price JC, Mayberg HS, Dannals RF, Wilson AA, Ravert HT, Sadzot B, et al. (1993): Measurement of benzodiazepine receptor number and affinity in humans using tracer kinetic modeling, positron emission tomography, and [^{11}C]flumazenil. *J Cereb Blood Flow Metab* 13:656-67.

37. Kugaya A, Sanacora G, Verhoeff NP, Fujita M, Mason GF, Seneca NM, et al. (2003): Cerebral benzodiazepine receptors in depressed patients measured with [^{123}I]iomazenil SPECT. *Biol Psychiatry* 54:792-9.

38. Blomqvist G, Pauli S, Farde L, Eriksson L, Persson A, Halldin C (1990): Maps of receptor binding parameters in the human brain--a kinetic analysis of PET measurements. *Eur J Nucl Med* 16:257-65.

39. Savic I, Blomqvist G, Halldin C, Litton JE, Gulyas B (1998): Regional increases in [^{11}C]flumazenil binding after epilepsy surgery. *Acta Neurol Scand* 97:279-86.

40. Mans AM, Kukulka KM, McAvoy KJ, Rokosz NC (1992): Regional distribution and kinetics of three sites on the GABA$_A$ receptor: lack of effect of portacaval shunting. *J Cereb Blood Flow Metab* 12:334-46.

41. Millet P, Graf C, Buck A, Walder B, Westera G, Broggini C, et al. (2000): Similarity and robustness of PET and SPECT binding parameters for benzodiazepine receptors. *J Cereb Blood Flow Metab* 20:1587-603.

42. Watabe H., Carson RE, Iida H (2000): The reference tissue model: three compartments for the reference region. *NeuroImage* 11:S12.